Microsystem Technologies 8 (2002) 375–382 © Springer-Verlag 2002
DOI 10.1007/s00542-002-0172-z

Modeling and controlling flow-induced suspension-head unit vibrations in hard disk drives

J. A. C. Humphrey, H. Haj-Hariri, T. Iwasaki, M. Kazemi, L. Rosales

Abstract The problem of flow-induced vibrations of suspension-head units (SHUs) in hard disk drives is investigated numerically. Attention is focused on the simplest geometrical and dynamical conditions that retain the physics essential to SHUs in real drives. Conservation equations are solved for the constant property, two-dimensional, unsteady flow of air past a pair of prisms contained in a channel with sliding walls. Each prism simulates the suspension section of a SHU. The prisms face each other symmetrically and are aligned parallel to the sliding channel walls, normal to their direction of motion. The sliding channel walls simulate the rotating disks in a drive. The flow fields obtained are used to calculate SHU vibration frequencies. For this, the suspension section of a SHU is approximated as an Euler–Bernoulli beam (linear motion) of constant ⌊⌋-shaped cross-section (henceforth denoted as "U-shaped") with a point mass, representing the magnetic head, located at its tip. The beam is assumed to be very stiff, meaning that movements near the design point (away from resonances) are small. This allows reliable solutions to be obtained by treating the flow as being unaffected by the miniscule motions of the suspensions, whereas the suspensions are fully affected by the unsteadiness imparted to them by the flow. SHU vibration characteristics have been determined relative to the flow fields that induce them for a variety of conditions. The paper discusses a subset of these for a flow at 50 m/s as well as the possible adaptation of interactive computational-experimental methodologies (ICEME) to minimize and/or control flow-induced vibrations of SHUs in hard drives.

Received: 28 August 2001/Accepted: 17 December 2001

J. A. C. Humphrey (✉), H. Haj-Hariri, T. Iwasaki, M. Kazemi
Department of Mechanical and Aerospace Engineering,
122 Engineer's Way, P.O. Box 400746,
Charlottesville, Virginia 22904-4746, USA
e-mail: jach@virginia.edu

L. Rosales
Phoenix Analysis and Design Technologies,
1465 N. Fiesta Boulevard, Suite 107,
Gilbert, Arizona 85233, USA

JACH gratefully acknowledges funding received from the National Storage Consortium Industry in support of this investigation. Special thanks go to Robert Evans of Hutchinson Technology and Alexei Sacks of Seagate Technology for helpful discussions and guidance on the topic of flow-induced suspension-head vibrations in hard drives.

1
Introduction

1.1
The problem of interest

Disk speed of rotation and track information density have the potential for increasing to remarkable values in the magnetic storage industry. Current magnetic storage technology is aimed at producing hard drives with disk speeds of rotation ranging from 7,200 rpm (desktop) to 15,000 rpm (server), area densities ranging from 20 Gb/in^2 (server) to 31 Gb/in^2 (desktop), track densities ranging from 40 ktpi (server) to 55 ktpi (desktop), and magnetic head (slider) flying heights less than 10 nm. Unfortunately, problems associated with magnetic head positioning error are seriously compounded at these speeds of rotation, thus limiting the practical implementation of the design target values. In particular, flow-driven suspension-head unit (SHU) vibrations have significant potential for adversely affecting head positioning control (Yamaguchi et al., 1986, 1990; Tokuyama et al., 1991; Humphrey et al., 1991; Abrahamson et al., 1991).

The dynamics and control of SHUs have been investigated extensively (Ono et al., 1999; Sasaki et al., 1999; Jeong et al., 1998). The servo loop for track positioning control includes the voice coil motor, actuator arm, suspension and magnetic head. Its bandwith is currently limited to about 1200 Hz for desktops and 1500 Hz for servers. The low resonance frequency of a suspension further limits the bandwith of the actuator servo system, and hence the track density that can be achieved in practice. As a consequence, the challenge is to design a SHU with sufficient compliance to allow the physical displacements required for the head to "fly" while providing enough stiffness to increase the natural frequency of the unit relative to the track positioning control.

This communication concerns an ongoing investigation aimed at understanding some of the flow conditions affecting magnetic head positioning error as a consequence of flow-induced SHU vibrations. Other important sources of positioning error such as spindle non-repeatable run-out (Ohmi et al., 1998) and flow-induced disk flutter (Imai et al., 1998; Shimizu et al., 2001) are not considered. The study also explores the use of interactive computational-experimental methodologies (ICEME) (Humphrey et al., 1993) to minimize and/or control these vibrations.

As will be shown, a two-dimensional (2D), unsteady analysis of the flow coupled (one-way) with a simple Euler–Bernoulli beam model for the SHU yields physically

realistic and highly insightful results. The simplicity of the beam model allows a self-consistent investigation of the effect of fluid forces on the SHU, something that has not been sufficiently explored to date. While a full finite element calculation of the SHU is certainly possible, when coupled to the flow field forces acting on it the calculation time- and space-resolution requirements render the problem practically intractable, in a reasonable amount of time, with current computer capabilities.

In spite of the simplicity of the SHU model investigated here the approach is entirely self-consistent, an important consideration. Our findings strongly support and extend earlier observations suggesting that SHUs are susceptible to flow-induced vibrations, especially for values of SHU resonance frequencies overlapping with corresponding energetic flow oscillations. Aside from its fundamental interest, the analysis yields generally applicable results of value for the improved design of hard drives within the context of an ICEME control approach.

1.2 Prior work

Two reviews (Humphrey et al., 1991; Abrahamson et al., 1991) discuss some of the early problems associated with flow-structure interactions in disk drives. The drives of current computers and servers are smaller, more compact, and rotate at much higher angular velocities, than those reviewed. Interestingly, however, the upper limit for the Reynolds number of the inter-disk flow, defined as $\mathrm{Re} = \Omega RH/\nu$ (where Ω is disk angular velocity, R disk radius, H inter-disk spacing and ν kinematic viscosity of air), has remained bounded, the increases in Ω being offset by the decreases in R and H. Notwithstanding, several major flow-structure interaction problems remain unsolved. Of these, the flow-induced vibrations of SHUs are particularly problematic given the much smaller mechanical tolerances required in current drive designs. Thus, we are especially concerned with experimental and analytical or numerical investigations relating to: (a) the physics of the flow past one or two suspension-like obstructions located in a passage with sliding walls or between rotating surfaces; (b) the physics of the flow-induced vibrations of such obstructions.

Several investigations have been performed for the flows around real SHUs as well as idealized suspension-like prisms of rectangular cross-section, with and without taper, in channels with sliding walls or between rotating disk surfaces (Humphrey et al., 1991; Abrahamson et al., 1991; Arnal et al., 1991; Hudson et al., 1991; Tzeng et al., 1991; Usry et al., 1993; Gor et al., 1994; Suzuki et al., 1997; Tatewaki et al., 2001). All of these studies consider single prisms with their longitudinal axes oriented normal to the direction of motion of the moving surface(s) that drive fluid motion. Nevertheless, the studies suggest that, provided the ratio of prism width (b, dimension parallel to moving surface) to height (a, dimension normal to moving surface and its direction of motion) is $b/a > 8$, and that the ratio of prism length to width is $L/b > 10$, the bulk of the flow immediately around the prism is strongly 2D. In contrast, the flow downstream of the prism quickly evolves into a highly 3D state of motion for the values of Re of interest. Also, the flow around the prism and immediately in its wake is highly unsteady as the result of vortex shedding. While at fixed Re vortex shedding is generally tuned to one or more preferred frequencies associated with the predominant 2D vortical structures, the energy in these structures is eventually distributed over a wide range of frequencies by the emerging smaller scales of motion.

We are unaware of any study in the open literature dealing with the flow past two suspension-like prisms contained between a pair of sliding or rotating surfaces. Consequently, in a separate study (Rosales et al., 2002), we have performed computer-intensive, unsteady, 3D numerical calculations of the flow past a pair of SHUs (of 3D geometry corresponding to the 2D geometry discussed below) for $\mathrm{Re} = 2500$ and 5000, approximately. The SHUs explored have tapered, U-shaped suspensions that are radially aligned and symmetrically oriented with respect to the midplane between a pair of corotating disks attached to a hub in an axisymmetric enclosure. The effect on the flow due to the E-block supporting the suspensions and the presence of a magnetic head on each suspension are also included.

These 3D results support the notion of a primarily 2D state of motion immediately around each suspension, primarily along a length removed from the interfering end effects of the E-block and the magnetic head. They also suggest that while the flow downstream of the suspensions is strongly unsteady, multi-scaled and 3D, much of that motion is gradually streamlined by the recirculating cross-stream flow in the bulk of the inter-disk space that is driven by the disk Ekman layers. Thus, in spite of the disturbing effects of the E-block and magnetic head, and of the presence of a relatively small region of streamwise (circumferential) flow reversal downstream of the SHUs (surrounding about 50% of the hub and located very near to it), the character of the flow approaching the upstream edges of the suspensions is similar to that between a pair of unobstructed corotating disks. Further evidence for this centrifugally-driven flow streamlining is evident in several of the single-prism studies (Tzeng et al., 1991; Usry, 1993; Gor, 1994; Suzuki, 1997).

The vibration dynamics of SHUs has been the subject of intense research and finite element methods are now used routinely to calculate the various modes (cantilever, bending, sway, torsion) of suspension vibrations (Zeng et al., 1998; Hatch, 2001). Notwithstanding, because of the large ranges in (and disparities between) the time and space scales of the vibrations and fluids phenomena, comparatively little has been done to model and calculate the effects of fluid forces on SHU vibrations. A notable exception is the pioneering work of Tokuyama et al. (1991). Using an LES technique, these authors calculate the unsteady, 2D flow around a single Watrous-type (U-shaped) suspension in a channel with sliding walls for $\mathrm{Re_C} = 3000$ ($\mathrm{Re_C}$ defined below). The drag and lift forces obtained at three cross-sections along the length of the tapered suspension are used to drive SHU motion. Calculations of SHU vibration frequencies are in good agreement with the first and second bending modes of the suspension. Similarly, calculations of head flying height and position fluctuations are in fairly good agreement with

corresponding measurements. From this and earlier work (Yamaguchi et al., 1986, 1990), the authors conclude it is the broad band energy in the turbulent-like unsteady flow around a suspension, especially that generated by shearing forces at its front and back edges, that induces a SHU to vibrate at its lower natural frequencies, and that these frequencies need not coincide with the predominant vortex shedding frequencies of the suspension.

1.3
Objectives of this investigation

Our continuing investigation has three interrelated objectives: (i) to calculate the unsteady, 2D flow around a pair of symmetrically-oriented suspension-like prisms contained in a channel with sliding walls; (ii) to model and predict the drag-, lift-, and torsion-induced vibration characteristics of the suspension pair, including the mass loading on each suspension due to its magnetic head; (iii) to use these results to explore the possible application of an ICEME approach to minimize and/or control the vibrations of SHUs in disk drives. With respect to objectives (i) and (ii), our approach is inspired by and extends the elegant work of Tokuyama et al. (1991).

Because of their considerable time- and memory-consuming nature, we have eschewed full 3D numerical calculations of the flows around geometrically complex SHUs. Instead, and because preliminary 3D calculations support the notion of a strong 2D flow around the suspensions in a disk drive, we have pursued a 2D calculation approach. The justifications for this are that: (a) much of the fluid and vibration physics relevant to SHUs can be explored via 2D calculations of the flow field; (b) if necessary, 2D flow results can be combined to yield quasi-3D flow fields; (c) for ICEME demonstration purposes, 3D flow calculations are not warranted.

Although we have calculated the flow fields corresponding to two suspension-like prism cross-sections (rectangular and U-shaped), for three flow velocities (25, 50 and 100 m/s), using two sets of inlet/exit channel flow boundary conditions (developing and periodic), space limitations restrict this communication to a subset of significant results for one of the cases explored. Likewise, while we recognize the importance of modeling and calculating lift- and torsion-induced modes of suspension vibration, this is beyond the scope of the present study where we have focused on drag-induced vibrations. Two more detailed communications (Rosales et al., 2002; Kazemi et al., 2002) are in preparation.

2
Flow field model and results

2.1
Geometry

For purposes of the fluid flow calculations we refer to Fig. 1. This shows instantaneous pictures of the vorticity and pressure fields obtained for the flow past a pair of suspension-like prisms in a 2D channel with sliding walls. In these and all other flow field calculations, the suspension portion of a SHU, that is, the U-shaped beam fixed to the E-block and supporting the magnetic head, is assumed to be the only significant part of the structure interacting with the flow. The sliding walls simulate the rotating surfaces of a pair of disks in a real drive.

It is also assumed that the vibration amplitudes of the suspensions are sufficiently small that their motions do not contribute significantly to the structure and dynamics of the flow. This one-way coupling assumption greatly simplifies the computational effort and is justified by the smallness of the vibration amplitudes the hard disk drive industry is prepared to accept (less than a few nanometers or, equivalently, less than 0.01% of the suspension width). Should the SHU model ever predict vibration amplitudes that would affect the flow (so as to invalidate the one-way coupling assumption), these would be so large as to be unacceptable from the design point of view. In this event, the present model is still useful in that it can identify unacceptable designs.

The channel is of length $L_C = 12$ mm and height $H_C = 2.0$ mm. Its walls slide at velocity $U_C = 50$ m/s along their length. This yields Re_C $(=U_C H_C/\nu) \approx 4000$ using ($\nu = 15.8 \times 10^{-6}$ m^2/s for air at 300 K). The suspensions are U-shaped prisms of constant cross-section and they are symmetrically oriented with respect to the channel midplane. For each prism, the width is $b = 2.0$ mm, the edge height is $a = 0.20$ mm and the thickness around the U-shape is $t = 0.10$ mm. The prisms face each other along the open sides of their U-shapes, the closed side of each prism being located at a distance $g = 0.40$ mm from its corresponding channel wall. The upstream edges of both prisms are located a distance $y = 3.0$ mm from the channel inlet flow plane.

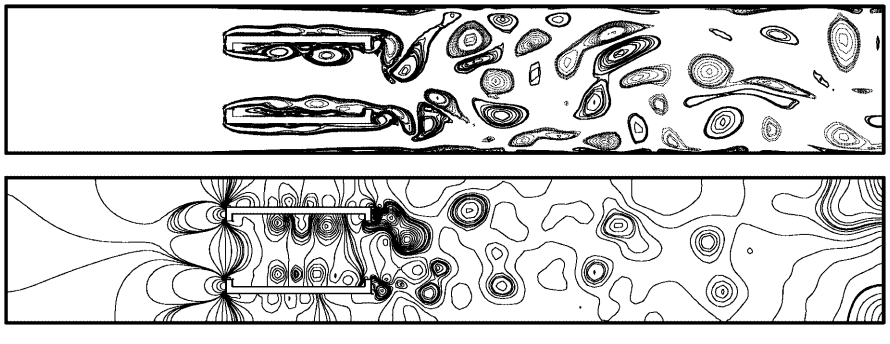

Fig. 1. Instantaneous vorticity (top) and pressure (bottom) fields for a pair of U-shaped suspension-like prisms in a channel with uniform inlet and sliding wall velocities at 50 m/s ($Re_C = 4000$). Fluid and wall motion are from left to right. Coordinates: y along channel length, z transverse to channel length, x normal to plane of paper

2.2 Conservation equations, boundary conditions and numerical solution

The flow field is described by unsteady, 2D, constant property forms of the momentum and continuity equations. These are solved numerically subject to the following initial and boundary conditions: (a) flow starting from rest, evolving to "statistically stationary" state; (b) impermeable, no-slip velocity boundary conditions along all solid surfaces; (c) uniform flow at the channel inlet plane, moving at the velocity of the channel walls ($U_O = U_C$); (d) developed flow at the channel exit plane. An algebraic system of finite difference equations is obtained by volume integration of the conservation equations over staggered control volumes for the velocity components and pressure, respectively. The third-order QUICK scheme is used to approximate convection terms and second-order central differencing to approximate diffusion. A fully implicit, second-order, three-level scheme is used for time.

Numerical solutions are obtained using the FAHTSO code (Rosales et al., 2001). This incorporates an adaptation of the SIMPLE algorithm to obtain velocity and pressure. The modified strongly implicit procedure is used to solve the system of algebraic equations. The grid spacing and time steps employed in the present calculations are set by reference to the extensive study of these effects for similar calculations (using the same code) of flows past square prisms in 2D channels with fixed walls, performed by Rosales, 2001). The present calculations are performed on a 180×124 (y, z) non-uniform grid using a time step of 1.25×10^{-7} s. (This grid is the most refined we could use to complete the volume of calculations performed in a reasonable amount of time. A typical run time on a DELL 620 computer with dual 933 MHz Pentium III processors takes about 75 h for a converged solution corresponding to a physical time record about 10 s long.) We estimate that the accuracy of the computed flow fields lies within 5% of grid-independent results. Further details concerning the numerical procedure are provided in Rosales et al. (2001).

2.3 Flow field results and discussion

The numerical results reveal a highly non-linear, unsteady flow. Instantaneous values of the vorticity and pressure fields are shown in Fig. 1 for a pair of U-shaped suspension-like prisms. Detailed inspection of these results reveals: (I) at the upstream edge of each prism: (a) flow separation and reattachment along the closed side of the prism; (b) flow separation and vortex shedding along the open side of the prism; (II) at the downstream edge of each prism: (a) alternating vortex shedding along the closed and open sides of the prism; (b) strong interactions between vortices along the open sides of the prism.

Both drag and lift coefficients are obtained. Typical (simultaneous) time records of the total drag coefficients $C_D[= (F_d/a)/(1/2\rho_f U_O^2)]$; F_d aligned in the y-direction in Fig. 3] for the top and bottom prisms are plotted in Fig. 2. The differences between the mean and rms values for C_D given in the caption illustrate that even over relatively long time periods (relative to the largest flow oscillation periods), the average characteristics of the flow past a symmetrically oriented pair of prisms in a channel are not necessarily symmetrical themselves with respect to the channel mid-plane. The spectrum for C_D corresponding to the bottom prism is shown in Fig. 4. Given the clean nature of the flow approaching the pair of prisms, it is clear that the fluctuations in drag experienced by a prism are associated with the vortices shed by it as affected by the vortices shed by the other prism.

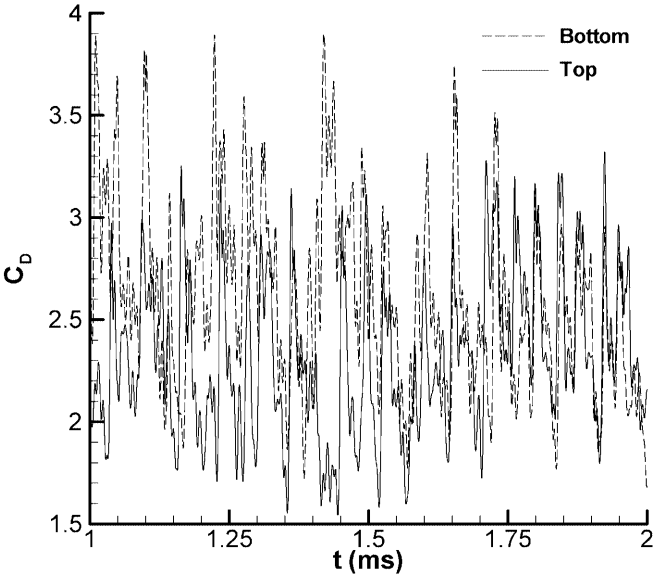

Fig. 2. Simultaneous time records of the total drag coefficients for each of a pair of prisms corresponding to the flow in Fig. 1. Top prism: $C_{Dave} = 2.36$, $C_{Drms} = 0.48$; bottom prism: $C_{Dave} = 2.52$, $C_{Drms} = 0.51$

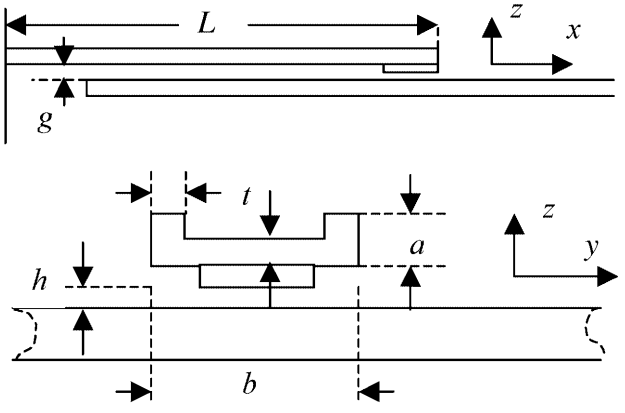

Fig. 3. Side view (top) and end view (bottom) of an idealized SHU (one of a pair as described in the text) located above a surface moving in the y-coordinate direction. Relevant dimensions are given in the text. Drawing is not to scale

3 Suspension-head model and results

3.1 Geometry

For purposes of the drag-induced vibration calculations, each of the two suspension-like prisms between the sliding

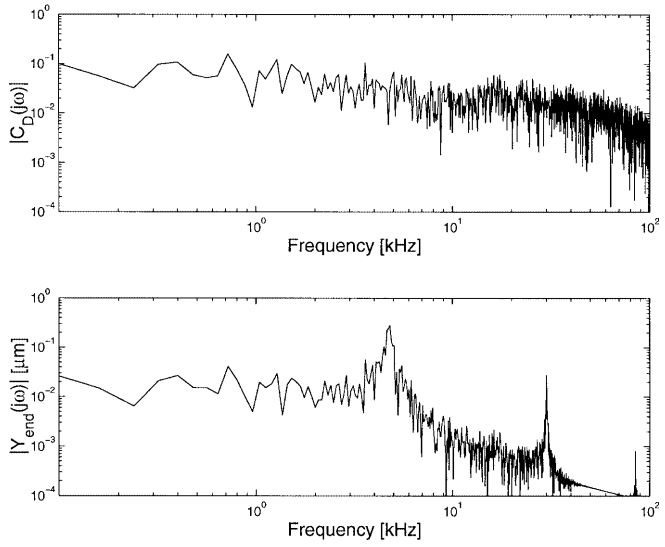

Fig. 4. C_D (top) and Y_{end} (bottom) spectra for the bottom SHU of a pair in a channel flow at 50 m/s

channel walls is approximated as an Euler–Bernoulli beam of constant U-shaped cross-section, with a magnetic head suspended from its free end. Figure 3 provides side (*x-z* plane) and end (*y-z* plane) views of the SHU geometry modeled. The end view corresponds to a *y-z* plane passing through the magnetic head. It is important to note that for purposes of calculating the beam dynamics the head is modeled as a point source of mass. However, for purposes of calculating the contributions to drag due to friction between the head and the sliding surface, the head is given a finite surface area $A_{MH} = 1.25$ mm^2. The length of the beam is $L = 18$ mm and its other dimensions are as given in Sect. 2.1. Each beam is assumed to be rigidly fixed at its base (to what would be the E-block). A hydrodynamic lubrication layer of thickness h allows the head to "fly" over the sliding surface.

3.2
Beam equation, boundary conditions and numerical solution

We are concerned here with the drag-induced motions of the beam in the *y*-coordinate direction, parallel to the sliding channel surface and its motion. (Lift- and torsion-induced beam motions can be treated similarly, but this is beyond the scope of the present work.) The dimensional linear equation and boundary conditions describing the motion of the beam about its average displaced location, and the idealizations invoked to obtain the beam equation, are given below. A detailed derivation is available in Kazemi et al. (2001).

$$\rho A\ddot{Y} + \rho_f U(x)[C_{Dave} + c_D(t)]\dot{Y} + EI\frac{\partial^4 Y}{\partial x^4} = \frac{1}{2}\rho_f a U^2(x) c_D(t) \quad (1)$$

$$Y(0,t) = 0, \quad \frac{\partial Y}{\partial x}(0,t) = 0, \quad \frac{\partial^2 Y}{\partial x^2}(L,t) = 0, \quad F_C + EI\frac{\partial^3 Y}{\partial x^3}(L,t) = M\ddot{Y}(L,t) + A_{MH}\frac{\mu_f}{h}\dot{Y}(L,t) \quad (2)$$

In these expressions: a, A, ρ, E and I are the edge height, cross-sectional area, density, Young's modulus and moment of inertia of the beam (stainless steel); M (= 1.6845×10^{-6} kg) is the (point) mass of the magnetic head at $x = L$, and A_{MH} its area at distance h from the moving surface; ρ_f and μ_f are the density and dynamic viscosity of air; C_{Dave} and $c_D(t)$ are the average and fluctuating components of C_D due to the drag forces acting on the beam; $U(x)$ is the x-distribution (along the beam) of the approaching fluid velocity; Y is the displacement of the beam at arbitrary x in the y-coordinate direction. The quantity F_C is a controlling force, explained below. For the analysis in this section $F_C = 0$.

The following can be shown (Kazemi et al., 2002): (a) virtual mass effects are negligible in air; (b) viscous damping by the lubrication layer supporting the magnetic head is negligible for thicknesses $h > 1$ nm, approximately; (c) one-way flow-to-beam forcing can be assumed due to the large stiffness of the beam; (d) similar equations can be derived for the lift- and torsion-induced motions of the beam.

Finite difference approximations to Eqs. (1) and (2) are obtained using second order central differencing for both the time and space terms. The resulting finite difference form for Eq. (1) is implicit in time. Its application to points along the beam yields a system of algebraic equations that are solved in time using Gaussian elimination. The space and time steps used are $\Delta x = L/(200 - 1)$ mm and $\Delta t = 10^{-9}$ s. Because the time step for the beam calculations is much smaller than that for the flow calculations, linear interpolation is used to obtain the values of $c_D(t)$ needed to solve the beam equation. A typical run time on a DELL 620 dual processor computer is approximately 10 h for a solution corresponding to a c_D *(t)* time record 1.25×10^{-2} s long. Further details are provided in Kazemi et al. (2002).

3.3
Vibration results and discussion

Present results are for a constant, uniform approaching velocity of $U(x) = U_O = 50$ m/s with C_{Dave} and $c_D(t)$ prescribed from the flow calculations. A typical time record for the displacement of the free end of the bottom beam, Y_{end}, is shown in Fig. 6b, discussed below. At this velocity we find that the average rms of the displacement of the free end of either beam is $Y_{rms} = 445.5 \pm 63.5$ nm. (Note: at 25 m/s we find $Y_{rms} = 35.2 \pm 3.1$ nm.) Figure 4 shows the spectra for C_D and Y_{end} of the bottom beam and very similar results are obtained for the top beam. The resonance frequency of the beams occurs at about 4.7 kHz and, as already noted by Tokuyama et al. (1991), does not coincide with any of the fundamental vortex shedding frequencies or their harmonics. Thus, for the time period examined, the beams are driven by fluctuations in the drag force of frequency that fortuitously coincides with the beam's resonance frequency.

Our results also reveal a beat frequency between the two beams of about 66 ± 6.5 Hz. Given that the flow field is unaffected by the suspension vibrations (because of the assumed one-way fluid-to-suspension coupling), it is clear that the observed asymmetric SHU vibration behavior is

due to flow field asymmetries. The origin of such asymmetries lies in the interaction of the flow with the stationary suspensions in its path (Rosales et al., 2001; Kazemi et al., 2001).

4
ICEME approach to control SHU vibrations

In the ICEME research approach the key notion is: "to pool relatively sparse measured and calculated data bases for a particular problem to create a composite data base richer in total information content than its constituents separately (Humphrey et al., 1993)." Judiciously chosen, the combined data base should help accelerate problem solving. To demonstrate the principle, the numerical models used to calculate the flow and SHU physics are taken here as the "laboratory experiment" to be controlled via the ICEME approach.

Our objective is to use fluid mechanics information to reduce the flow-induced vibrations of SHUs by feedback control for higher tracking accuracy. Physically, what we wish to do is add a controlling force, F_C , to the left hand side of the fourth boundary condition in Eqs. (2). We assume that actuation and sensing mechanisms are available to generate F_C at the suspension tip, and to measure the tip displacement Y_{end}. Our target performance is a track density of 55 ktpi (track pitch = 0.46 μm) with a disk speed of rotation corresponding to 15,000 rpm ($U_O = 50$ m/s). For illustration, we consider the control of the bottom SHU only.

Analysis of the flow shows that the drag force, $F_d(t)$, behaves like white noise; see Fig. 6a. Indeed, analysis confirms that $F_d(t)$ has a roughly flat spectrum over the frequency range of interest. Hence we choose to model the drag force as a zero-mean white noise process in our control design. Calculating the standard deviation from the time domain data, we find

$$\sqrt{E[F_d(t)^2]} = 0.149 \text{ N/m}$$

where $E[\bullet]$ is the expectation operator. We also assume the sensor noise $V(t)$ at the free end of the suspension to be white noise with the following standard deviation:

$$\sqrt{E[V(t)^2]} = 0.025 \text{ μm} \ .$$

We design a linear controller $F_C = K(s)\ (Y_{end} + V)$ that minimizes the variance of the tip displacement Y_{end} in response to the drag force and sensor noise, with a reasonable magnitude of the control force. The control design problem can be formulated as follows:

$$\min_{K(s)} \{[E[F_C(t)^2] + q^2 E[Y_{end}(t)^2]\}$$

where q is a design weight. This optimization problem falls into the framework of the linear quadratic Gaussian (LQG) control theory and can be solved exactly.

We start our design based on the 200th order linear model $P(s)$ of the SHU obtained by spatial discretization into 100 points over the interval $0 \le x \le L$ with 6th order polynomial approximations of Y. Balanced model reduction is performed to obtain a reduced order model $P_r(s)$ of 6th order. We design an optimal LQG controller based on $P_r(s)$ then evaluate the closed-loop performance by simulation of the higher order model $P(s)$. After some trial and error, an appropriate value of the design weight is found to be $q = 6$ mN/μm.

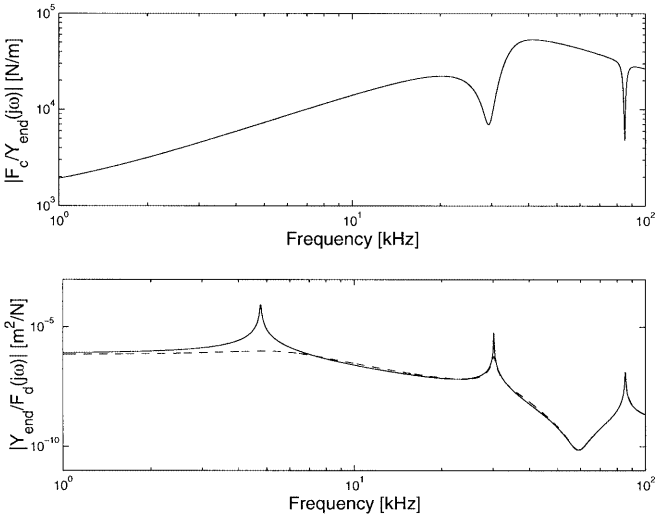

Fig. 5. Controller frequency response (top) and SHU frequency response (bottom) with (dashed line) and without (solid line) control. Results are for the bottom beam of a pair in a channel flow at 50 m/s

Based on the design procedure described above, we find a 6th order controller whose bode magnitude plot is shown in Fig. 5a. We see that the dynamic controller is acting as a differentiator in the frequency region around the first mode 4.76 kHz so that the effective velocity feedback adds damping to the first mode. As a result, the first mode is well damped in the closed-loop, which can be seen in Fig. 5b where the dashed and solid curves give frequency responses of the SHU with and without control, respectively. The same approach does not work for the second and the third modes because their natural frequencies (30.2 and 85.3 kHz) are much higher than the first and hence a large control bandwidth would be required. Thus, instead, the controller places notch filters at these frequencies to avoid exciting these modes.

The simulation results of the time responses are provided in Fig. 6 where the 200th order model $P(s)$ is used for the SHU. Without control, the tip displacement Y_{end} vibrates due to the drag force F_d; see Fig. 6b. With the feedback controller, the vibration amplitude reduces from a peak value of 1.27 μm to a peak value of 0.21 μm; see Fig. 6c. The required control force to achieve this is in the order of 1 mN; see Fig. 6d.

While current actuator/sensor technology may not allow for the actual implementation of our controller at the present moment, our findings demonstrate what it would take, approximately, to achieve 55 ktpi at 15,000 rpm.

5
Conclusions

Numerical calculations have been performed for the unsteady flow and vibration characteristics of a pair of SHUs

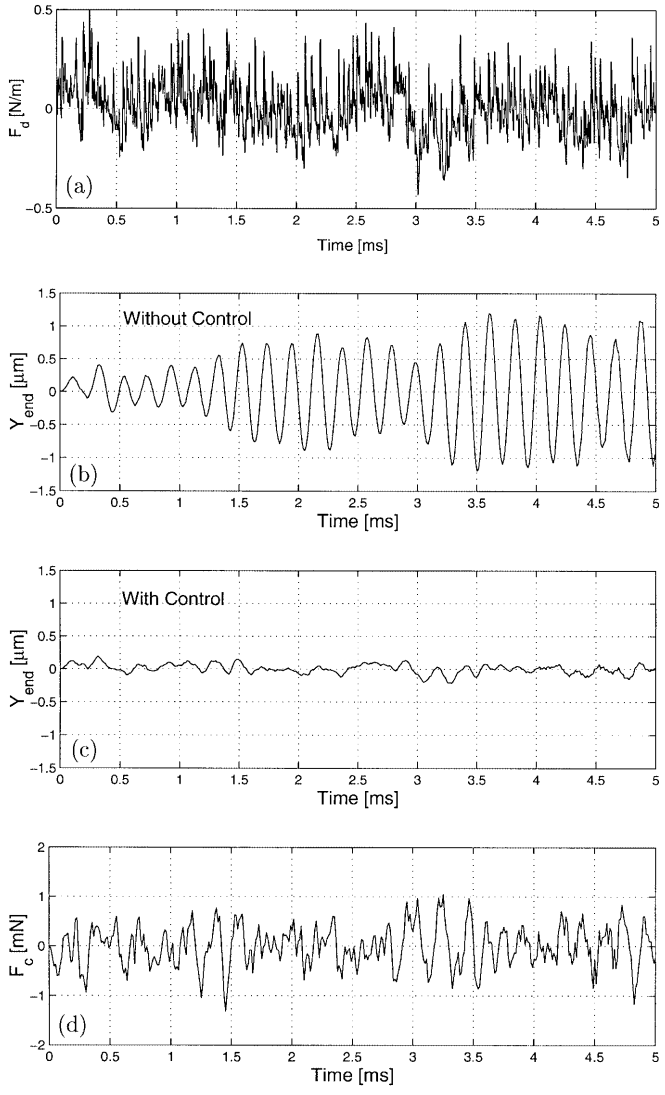

Fig. 6a–d. Time responses for a SHU corresponding to the bottom beam of a pair in a channel flow at 50 m/s

under idealized but physically meaningful conditions. The results obtained are in broad agreement with earlier observations. However, the present, more detailed calculations reveal asymmetric flow behavior resulting from the suspensions that influences the vibration characteristics of the SHUs. Using the flow and vibration numerical models as the equivalent of the "laboratory experiment" in an ICEME research approach, it is shown that *real-time* knowledge of the drag forces acting on SHUs could, in principle, be used to significantly minimize their vibrations. The results obtained are especially encouraging and the possibility of such advanced fluid information control should be investigated in the physical laboratory.

References

Abrahamson SD; Chiang C; Eaton JK (1991) Flow structure in head-disk assemblies and implications for design. In: Bhushan B (ed) Adv Info Storage Sys, vol. 1, pp. 111–132

Arnal M; Goering D; Humphrey JAC (1991) Vortex shedding from a bluff body adjacent to a plane sliding wall. J Fluids Eng 113: 384–398

Gor D; Humphrey JAC; Greif R (1994) Ventilated flow between corotating disks with large obstructions in a fixed cylindrical enclosure. J Fluids Eng 116: 828–834

Hatch MR (2001) Vibration Simulation Using MATLAB and ANSYS, Chapman and Hall/CRC, Boca Raton

Hudson AJ; Eibeck PA (1991) Torque measurements of corotating disks in an axisymmetric enclosure. J Fluids Eng 113: 648–653

Humphrey JAC; Chang CJ; Li HW; Schuler CA (1991) Unobstructed and obstructed rotating disk flows: a summary review relevant to information storage systems. In: Bhushan B (ed) Adv Info Storage Sys, vol. 1, pp. 79–110

Humphrey JAC; Devarakonda R; Queipo N (1993) Interactive computational-experimental methodologies (ICEME) for thermofluids research: applications to the optimized packaging of heated electronic components. In: Yang KT, Nakayama W (eds) Computers and Computing in Heat Transfer Science and Engineering, CRC Press and Begell House, Inc., New York, pp. 293–317

Imai S; Okazaki T; Mori K (1998) Flutter reduction by centrifugal airflow for high-rotation-speed disks. In: Bhushan B Ono K (eds) Adv Info Storage Sys, vol. 9, pp. 5–17

Jeong TG; Chun JI; Chung CC; Byun YK; Ro KC (1998) Measurement technique for dynamic characteristics of HDD head-suspension assembly in normal operating conditions. In: Bhushan B, Ono K (ed) Adv Info Storage Sys, vol. 9, pp. 47–61

Kazemi M; Haj-Hariri H; Iwasaki T; Humphrey JAC (2002) Flow-induced suspension-head vibrations in disk drives (Part II): suspension-head model and control results (in preparation)

Ohmi T; Itoh K (1998) Small NRRO spindle-motor with hydrodynamic bearings and a Pivot. In: Bhushan B, Ono K (eds) Adv Info Storage Sys, vol. 9, pp. 19–32

Ono K; Takekawa H; Yamaura H (1999) Inphase design of the two lowest natural modes of vibrations of swing-arm for a high frequency band head positioner. In: Bhushan B, Ono K (eds) Adv. Info Storage Sys, vol. 10, pp. 19–32

Rosales JL; Ortega A; Humphrey JAC (2001) A Numerical simulation of the convective heat transfer in confined channel flow past square cylinders: comparison of inline and offset tandem pairs. Int J Heat and Mass Transfer 44: 587–603

Rosales L; Herrero J; Humphrey JAC; Haj-Hariri H; Giralt F (2002) Flow-induced suspension-head vibrations in disk drives (Part I): flow field model and results (in preparation)

Sasaki M; Suzuki T; Usui T; Fufisawa F; Hirai H; Kobayashi M Application of neural network system for track-following control of a dual stage hard disk drive. In: Bhushan B, Ono K (eds) Adv Info Storage Sys, vol. 10, pp. 119–133

Shimizu H; Tokuyama M; Imai S; Nakamura S; Sakai K (2001) Study of aerodynamic characteristics in hard disk drives by numerical simulation. IEEE Trans Magn 37: 831–836

Suzuki H; Humphrey JAC (1997) Flow past large obstructions between corotating disks in fixed cylindrical enclosures. J Fluids Eng 119: 499–505

Tatewaki M; Tsuda N; Maruyama T (2001) An analysis of disk flutter in hard disk drives in aerodynamic simulations. IEEE Trans Magn 37: 842–846

Tokuyama M; Yamaguchi Y; Miyata S; Kato C (1991) Numerical analysis of flying-height fluctuation and positioning error of magnetic head due to flow induced by disk rotation. IEEE Trans. Magn 27: 5139–5141

Tzeng H; Humphrey JAC (1991) Corotating disk flow in an axisymmetric enclosure with and without a bluff body. Int J Heat and Fluid Flow 12: 194–201

Usry W; Humphrey JAC; Greif R (1993) Unsteady flow in the obstructed space between disks corotating in a cylindrical enclosure. J Fluids Eng 115: 620–626

Yamaguchi Y; Takahashi K; Fujita H; Kuwahara K (1986) Flow induced vibration of magnetic had suspension in hard disk drive IEEE Trans Magn 22: 1022–1024

Yamaguchi Y; Talukder AA; Shibuya T; Tokuyama M (1990) Air flow around magnetic-dead slider suspension and its effect on slider flying-height fluctuation. IEEE Trans Magn 26: 2430–2432

Zeng QH; Bogy DB (1998) Dynamic characteristics of a suspension assembly part 2: numerical analysis. In: Bhushan B, Ono K (eds) Adv Info Storage Sys, vol. 8, pp. 121–133